

## Coherence of an Optically Illuminated Single Nuclear Spin Qubit

L. Jiang,<sup>1</sup> M. V. Gurudev Dutt,<sup>1</sup> E. Togan,<sup>1</sup> L. Childress,<sup>1</sup> P. Cappellaro,<sup>2</sup> J. M. Taylor,<sup>3</sup> and M. D. Lukin<sup>1,2</sup>

<sup>1</sup>Department of Physics, Harvard University, Cambridge, Massachusetts 02138, USA

<sup>2</sup>Institute for Theoretical Atomic, Molecular and Optical Physics, Cambridge, Massachusetts 02138, USA

<sup>3</sup>Department of Physics, Massachusetts Institute of Technology, Cambridge, Massachusetts 02139, USA

(Received 9 July 2007; published 19 February 2008)

We investigate the coherence properties of individual nuclear spin quantum bits in diamond [Dutt *et al.*, Science **316**, 1312 (2007)] when a proximal electronic spin associated with a nitrogen-vacancy (N-V) center is being interrogated by optical radiation. The resulting nuclear spin dynamics are governed by time-dependent hyperfine interaction associated with rapid electronic transitions, which can be described by a spin-fluctuator model. We show that due to a process analogous to motional averaging in nuclear magnetic resonance, the nuclear spin coherence can be preserved after a large number of optical excitation cycles. Our theoretical analysis is in good agreement with experimental results. It indicates a novel approach that could potentially isolate the nuclear spin system completely from the electronic environment.

DOI: 10.1103/PhysRevLett.100.073001

PACS numbers: 37.10.Jk, 03.67.Lx, 71.55.-i

Nuclear spins are of fundamental importance for storage and processing of quantum information. Their excellent coherence properties make them a superior qubit candidate even in room temperature solids. Unfortunately, their weak coupling to the environment also makes it difficult to isolate and manipulate individual nuclei. Recently, coherent preparation, manipulation and readout of individual <sup>13</sup>C nuclear spins in the diamond lattice were demonstrated [1,2]. These experiments make use of optical polarization and manipulation of the electronic spin associated with a nitrogen-vacancy (N-V) color center in the diamond lattice [3–6]. This enables reliable control of the nuclear spin qubit via hyperfine interactions with the electronic spin.

In order to be useful for applications in scalable quantum information processing [3], such as quantum communication [7] and quantum computation [8], the quantum coherence of the nuclear spins must be maintained even when the electronic state is undergoing fast transitions associated with optical measurement and with entanglement generation between electronic spins. In this Letter, we investigate coherence properties of such an optically illuminated nuclear spin-electron spin system. We show that these properties are well-described by a spin-fluctuator model [9–12], involving a single nuclear spin (system) coupled by the hyperfine interaction to an electron [13] (fluctuator) that undergoes rapid optical transitions and mediates the coupling between the nuclear spin and the environment. We generalize the spin-fluctuator model to a vector description, necessary for single N-V centers in diamond [1], and make direct comparisons with experiments. Most importantly we demonstrate that the decoherence of the nuclear spin due to the rapidly fluctuating electron is greatly suppressed via a mechanism analogous to motional narrowing in nuclear magnetic resonance (NMR) [14,15], allowing the nuclear spin coherence to be preserved even after hundreds of optical excitation cycles. We further

show that by proper tuning of experimental parameters it may be possible to completely decouple the nuclear spin system from the electronic environment. The spin-fluctuator model discussed here for N-V centers can be generalized to other AMO systems (see Refs. [16,17] for the recent progress).

The essential idea of this work is illustrated in Fig. 1. We consider an individual nuclear spin system ( $I = 1/2$ , associated with a <sup>13</sup>C atom) that is weakly coupled to the electronic spin of an N-V center via the hyperfine interaction. The transitions between ground and optically excited electronic states are caused by laser light and spontaneous emission of photons. The strength of the hyperfine inter-

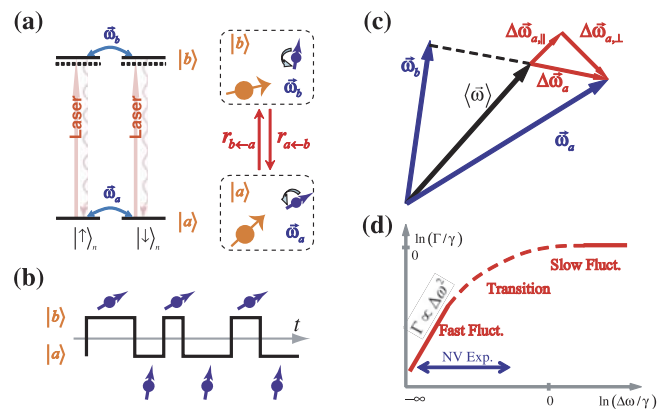


FIG. 1 (color online). (a) Energy levels (left) and schematic model (right) for optical transitions between different electronic states ( $|a\rangle$  and  $|b\rangle$ ), with transition rates  $r_{ba}$  and  $r_{ab}$ . The precession of the nuclear spin ( $\vec{\omega}_a$  or  $\vec{\omega}_b$ ) (blue arrow) depends on the electronic state ( $|a\rangle$  or  $|b\rangle$ ) (orange arrow). (b) Random telegraph trajectory of the electron, and time-dependent precession of the nuclear spin. (c) Geometric representation of Larmor precession vectors. (d) The decoherence rate  $\Gamma$  as a function of the differential precession frequency  $\Delta\omega$ , in units of  $\gamma$ .

action differs between the ground and the excited electronic states, because they have different spatial wave functions and thus different overlap with the nucleus. As the electron undergoes rapid optical transitions, the nuclear spin precesses according to a time-dependent effective magnetic field induced by the electron.

This situation can be modeled by considering the electron as a fluctuator with two states,  $|a\rangle$  and  $|b\rangle$ . Let us first assume that the incoherent transitions between these two electronic states  $|a\rangle \xrightleftharpoons[r_{ab}]{} |b\rangle$  are described by the random telegraph process as shown in Fig. 1(b), which is fully characterized by the classical transition rates  $r_{ba}$  and  $r_{ab}$  (corresponding to the optical pumping rate and the radiative decay rate, respectively, resulting from an off-resonant optical drive). The nuclear spin will undergo time-dependent precession, characterized by vectors  $\vec{\omega}_a$  and  $\vec{\omega}_b$  for the electronic states  $|a\rangle$  and  $|b\rangle$ , respectively [Fig. 1(a)].

In general, the precession vectors  $\vec{\omega}_a$  and  $\vec{\omega}_b$  may point along different directions as shown in Fig. 1(c). For example, the nuclear spin can precess around different axes for different electronic states. Furthermore, the electron undergoes fast optical transitions and introduces high frequency noise, which, in addition to dephasing, can induce spin flips [1]. Therefore, we need to consider the nuclear spin precession around a time-dependent, stochastic vector  $\vec{\omega}(t)$ , generalizing the earlier scalar model [11,12].

Let  $\gamma$  and  $\Delta\omega$  be the typical scales for the electron transition rates and the *difference* between the qubit precession vectors, respectively. Let us now consider the limiting case of a fast fluctuator ( $\gamma \gg \Delta\omega$ ). In this case we may use a perturbative approach associated with the small phase shift acquired by the nuclear spin during one excitation cycle  $\delta\phi \sim \Delta\omega/\gamma$ . On average this phase shift will result in a modification of the precession frequency. In addition, due to random variations in the time spent in different electronic states the phase shift will undergo a random walk with diffusion constant  $\sim \delta\phi^2\gamma \sim \Delta\omega^2/\gamma$ .

More precisely, to the first order, we have the average precession vector

$$\langle \vec{\omega} \rangle = \frac{r_{ba}^{-1} \vec{\omega}_a + r_{ab}^{-1} \vec{\omega}_b}{r_{ba}^{-1} + r_{ab}^{-1}}, \quad (1)$$

where the weights are proportional to the durations of different states for the fluctuator. As illustrated in Fig. 1(c),  $\langle \vec{\omega} \rangle$  defines the quantization axis of the spin system. The difference between the instantaneous precession vector ( $\vec{\omega}_a$  or  $\vec{\omega}_b$ ) and  $\langle \vec{\omega} \rangle$ ,  $\Delta\vec{\omega} = \vec{\omega}_a - \langle \vec{\omega} \rangle$  can be decomposed into the parallel and perpendicular components. The perpendicular component introduces spin flips along the quantization axis at rate  $\Gamma_{\perp} \sim (\Delta\omega)_{\perp}^2/\gamma$ . The parallel component causes stochastic phase accumulation, leading to dephasing at the rate  $\Gamma_{\parallel} \sim (\Delta\omega)_{\parallel}^2/\gamma$ . Note that both rates are inversely proportional to the fluctuator transition rate  $\gamma$  in the limit of fast electronic transitions. The

underlying physics is analogous to the motional narrowing of NMR [14], in which the rapid motion of the environment (corresponding to large  $\gamma$ ) averages out the randomly accumulated phase.

In the opposite slow-fluctuator limit ( $\gamma \lesssim \Delta\omega$ ), the decoherence rate is only determined by the fluctuator transition rates. For each fluctuator transition, there is a time variation,  $\delta t \sim 1/\gamma$ , which induces an uncertainty in the rotation  $\delta\phi \sim \Delta\omega\delta t \sim \Delta\omega/\gamma \sim 1$ . This implies that a single transition of the fluctuator is sufficient to destroy the coherence of the spin system. The resulting qualitative dependence of the nuclear spin decay upon difference in Larmor precession is illustrated in Fig. 1(d).

We now introduce the master equation formalism and illustrate that it is possible to reduce the system dynamics to a set of linear differential equations, even in the presence of the noncommutative stochastic precession. We will first solve the spin-fluctuator model with the two-state fluctuator described above. After that, we extend the procedure to include multistate fluctuators into the formalism.

The incoherent transition of the two-state fluctuator [Fig. 1(a)] can be described by the master equations

$$\frac{d}{dt} \begin{pmatrix} p_a \\ p_b \end{pmatrix} = \begin{pmatrix} -r_{ba} & r_{ab} \\ r_{ba} & -r_{ab} \end{pmatrix} \begin{pmatrix} p_a \\ p_b \end{pmatrix}, \quad (2)$$

where  $p_a$  and  $p_b$  are occupation probabilities for states  $|a\rangle$  and  $|b\rangle$ .

The Hamiltonian of the nuclear spin (depending on the state of the fluctuator) is  $H = |a\rangle\langle a| \otimes H_a + |b\rangle\langle b| \otimes H_b$ , with  $H_a = \vec{\omega}_a \cdot \vec{I}$  and  $H_b = \vec{\omega}_b \cdot \vec{I}$ .

Since there is no coherence between different fluctuator states, we may write the density matrix for the composite system as  $\rho = |a\rangle\langle a| \otimes \rho_a + |b\rangle\langle b| \otimes \rho_b$ , where

$$\rho_j = \begin{pmatrix} \rho_{j,11} & \rho_{j,12} \\ \rho_{j,21} & \rho_{j,22} \end{pmatrix}$$

for  $j = a$  or  $b$ . The unitary evolution of the density matrix  $\rho$  with Hamiltonian  $H$  can be decomposed into two uncoupled parts:  $\frac{d}{dt}\rho_j = -i[H_j, \rho_j]$  for  $j = a, b$ . In terms of the Liouville operator, the unitary evolution is

$$\frac{d}{dt} \vec{\rho}_j = \mathcal{L}_j \vec{\rho}_j, \quad (3)$$

where the density operator is represented by a column vector  $\vec{\rho}_j = (\rho_{j,11}, \rho_{j,12}, \rho_{j,21}, \rho_{j,22})^T$  and the Liouville operator by a matrix

$$\mathcal{L}_j \equiv \mathcal{L}[\vec{\omega}_j] \equiv (-i)(H_j \otimes \mathbf{I} - \mathbf{I} \otimes H_j^*), \quad (4)$$

for  $j = a, b$ . Notice that the transition matrix depends linearly on the precession vector, and such linearity implies  $\mathcal{L}[\vec{\omega}_a] + \mathcal{L}[\vec{\omega}_b] = \mathcal{L}[\vec{\omega}_a + \vec{\omega}_b]$ .

Combining the dynamics of the system and the fluctuator, we may write down the following master equations:

$$\frac{d}{dt} \begin{pmatrix} \vec{\rho}_a \\ \vec{\rho}_b \end{pmatrix} = \begin{pmatrix} \mathcal{L}_a - \mathbf{r}_{ba} & \mathbf{r}_{ab} \\ \mathbf{r}_{ba} & \mathcal{L}_b - \mathbf{r}_{ab} \end{pmatrix} \begin{pmatrix} \vec{\rho}_a \\ \vec{\rho}_b \end{pmatrix}, \quad (5)$$

where  $\mathcal{L}_a$  and  $\mathcal{L}_b$  describe the (slow) dynamics of the precession;  $\mathbf{r}_{ba} = r_{ba}\mathbf{I}_{4\times 4}$  and  $\mathbf{r}_{ab} = r_{ab}\mathbf{I}_{4\times 4}$  are associated with the (fast) incoherent optical transitions between electronic states, not affecting the nuclear spin.

We generalize to a multistate fluctuator, by introducing  $r_{ij}$  the fluctuator transition rate from state  $j$  to state  $i$ , and  $r_{jj} \equiv \sum_{i \neq j} r_{ij}$  the total transition rate from state  $j$  to all other states. For an  $N$ -state fluctuator, the generalized form for Eq. (5) is

$$\frac{d}{dt} \vec{\rho}_i = (\lambda \mathcal{L}_i - \mathbf{r}_{ii}) \vec{\rho}_i + \sum_{j \neq i} \mathbf{r}_{ij} \vec{\rho}_j \quad (6)$$

where  $\vec{\rho}_j = (\rho_{j,11}, \rho_{j,12}, \rho_{j,21}, \rho_{j,22})^T$  for  $j = 1, 2, \dots, N$ , and  $\mathbf{r}_{ij} = r_{ij}\mathbf{I}_{4\times 4}$ . When there are  $M$  fluctuators, with  $N_j$  states for the  $j$ th fluctuator, we can always reduce it to one composite fluctuator with  $N = \prod_{j=1}^M N_j$  states.

Given all the parameters  $\{\vec{\omega}_i\}$  and  $\{r_{ij}\}$ , we can solve  $\vec{\rho}_i(t)$  exactly from the above  $4N$  linear differential equations [Eq. (6)] with initial conditions for  $\{\vec{\rho}_i(0)\}$ . Finally, the density matrix of the nuclear spin system is  $\vec{\rho}(t) = \sum_i \vec{\rho}_i(t)$ , which together with Eq. (6) provides an exact solution to the generalized spin-fluctuator model.

The experimental procedure for probing the dynamics of an optically illuminated nuclear spin qubit proximal to N-V centers in diamond is described in detail in Ref. [1]. The N-V center is a spin triplet in the ground electronic state. In the experiment we optically polarize the electron into  $m_s = 0$ , in which the hyperfine interaction with the nuclear spin vanishes to leading order. Furthermore, it is believed [18], and is confirmed by experimental evidence reported below, that the electronic spin is a good quantum number during the optical excitation of the N-V center. Hence the electron should mostly remain in the  $m_s = 0$  manifold during optical excitation.

However, the hyperfine interaction with the electron can dramatically change the precession of the nuclear spin by modifying its effective magnetic moment [4]. The direction and magnitude of the precession vector, which is determined by the effective  $g$  tensor [4], varies due to the changes in the contact and dipolar interactions associated with different electronic states. Under these experimental conditions, the nuclear precession vectors associated with different electronic states should be proportional to the perpendicular components of the external magnetic field,  $B_{\perp}$ , with a proportionality constant and direction that depends upon the electronic state. Thus, we present the experimental data (Fig. 2) as functions of the ground state precession frequency  $\omega_g$  ( $\omega_g \propto B_{\perp}$ ), which can be accurately measured. Both the optically induced decoherence rate  $\Gamma$  (the decay rate of the nuclear spin Bloch vector) and the change in average Larmor precession frequency  $\langle \vec{\omega} \rangle - \omega_g$  were measured for a particular N-V center. For the presented data, the optical excitation rate was chosen to correspond to about one half of saturation intensity.

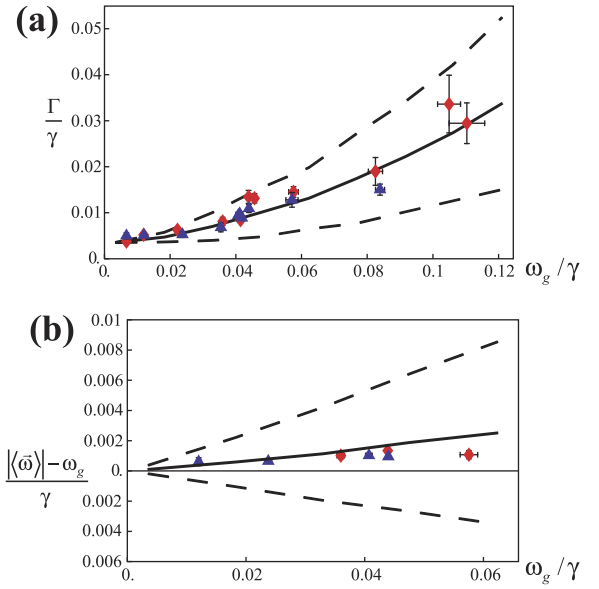


FIG. 2 (color online). Comparison between experimental data (points) and simulation (lines). (a) Optically induced decoherence rate  $\Gamma$  as a function of ground state Larmor precession frequency  $\omega_g$  (data adopted from Ref. [1]). (b) Shift of average Larmor precession frequency  $\langle \vec{\omega} \rangle - \omega_g$  as a function of  $\omega_g$ . For both plots, the axes are also labeled in dimensionless units, normalized by the radiative decay rate  $\gamma = 86 \mu\text{s}^{-1}$ . Experimental data points (blue triangles, red diamonds) include nuclear spins prepared along both directions ( $\hat{x}$ ,  $\hat{z}$ ) perpendicular to the Larmor precession vector ( $\hat{y}$ ). The full lines are from simulation of the generalized spin-fluctuator model, averaging over 50 different sets of randomly generated excited states, as described in the text. The simulation assumes  $N = 3$  for the fluctuator (i.e. one ground state and two excited states [19,20]). The dashed lines are the statistical standard deviation of the different realizations. In panel (a), the curves from simulation are manually shifted upwards by  $\Gamma_0 = 3.4 \times 10^{-3} \gamma$ , as described in the text.

A comparison between first-principle theory and experiment would require precise knowledge of nuclear precession vectors for both the *ground* and *excited* electronic states. The experiments, performed at room temperature, involve excitation of multiple excited states, whose wave functions are not known in great detail. To model quantum dynamics of such a system, we assume that the excited state precession vector has similar order of magnitude to that of the ground state, but might point along a different direction. In the following, we label the ground state as the first state of the fluctuator with precession frequency  $\vec{\omega}_g \equiv \vec{\omega}_1$  for the proximal nuclear spin. The  $j$ th excited state has precession vector  $\vec{\omega}_j$ , with its three components drawn from a normal distribution with mean 0 and deviation  $\sigma_\omega \sim \omega_g$ , for  $j = 2, \dots, N$ . We assume that the excitation rate from the 1st to the  $j$ th excited state  $r_{j1} = R/(N-1)$ , the radiative decay rate  $r_{1j} = \gamma = 86 \mu\text{s}^{-1}$  [19], and the total excitation rate  $R = \gamma$ . The transitions among excited states are neglected. According to [19,20], there are at least



two excited states involved in the optical transition, so we set  $N = 3$ . By choosing  $\sigma_\omega = 2.5\omega_g$ , we find good agreement between theory and experiment as shown in Fig. 2.

In the fast-fluctuating regime ( $\omega_g \ll \gamma$ ), the experimental decoherence rate increases quadratically with  $\omega_g$ , consistent with the scaling obtained from the fast-fluctuator limit. When the precession frequency becomes comparable to the fluctuator transition rates ( $\omega_g \lesssim 0.2\gamma$ ),  $\Gamma$  increases subquadratically with  $\omega_g$ . This is because we are in the transition region as indicated in Fig. 1(d). In principle, for even higher precession frequency, the decoherence rate should saturate at the optical transition rate. Experimentally, however, it is difficult to manipulate the nuclear spin for very high precession frequency ( $\omega_g > 0.2\gamma$ ) [1].

In addition to the electronic spin-conserving optical transitions analyzed above, the spin-changing transitions between  $m_s = 0$  and  $m_s = \pm 1$  may also induce decoherence of the nuclear spin. However, the hyperfine field from the electron in spin state  $m_s = \pm 1$  is oriented along the well-defined  $z$  axis [1], which introduces decoherence for nuclear spin state  $|\uparrow\rangle_X$ , but not for  $|\uparrow\rangle_Z$ . This contradicts the observation that the decoherence rates (with initial states  $|\uparrow\rangle_X$  and  $|\uparrow\rangle_Z$ ) are similar for the observed center (see Fig. 2). Therefore, we conclude that the spin-changing transitions should not be the dominant process for optically induced nuclear spin decoherence.

By extrapolating the experimental data to zero external magnetic field, we find that there is still a finite decoherence rate  $\Gamma_0 \approx 3.4 \times 10^{-3}\gamma$  [simulation curves are offset with additional fitting parameter in Fig. 2(a)]. Remarkably, these data indicate that the nuclear spin coherence is still maintained after scattering  $\gamma/\Gamma_0 \sim 300$  photons by the electron. This insensitivity, enabled via effects analogous to motional averaging, is of critical importance for the feasibility of N-V-center-based distant quantum communication [7] and distributed quantum computation [8] protocols.

The zero field decoherence rate  $\Gamma_0$  is still related to optical transitions, because it is much larger than the observed decoherence rate of the nuclear spin in the dark  $\Gamma_{\text{dark}} \approx 3 \times 10^{-4}\gamma$  [1]. We attribute this zero field decoherence to the orbital motion of the optically excited states, which produces a “residual” magnetic field at the position of the nucleus. The residual magnetic field can be present for optically excited states, because the orbital motion for these states is not quenched [19,20]. Considering the nucleus on the second coordination sphere with respect to the vacancy (i.e.,  $r \approx 2.6 \text{ \AA}$ ), the magnetic field from the orbital motion is approximately  $\mu_B/r^3 \approx 500\text{--}1000 \text{ G}$ . This gives an estimated decoherence rate  $\Gamma_0 \approx \Delta\omega^2/\gamma \approx (1\text{--}5) \times 10^{-3}\gamma$ , which is consistent with the value observed experimentally.

These observations may allow us to develop new methods to further suppress optically induced nuclear decay. Specifically, at low temperatures ( $T < 10 \text{ K}$ ), it is possible to resolve individual optical transitions and selectively

drive the electron between the ground state and one excited state. Under these conditions, it should be possible to eliminate the decoherence  $\Gamma_0$  by applying an external magnetic field that exactly compensates the residual field from the orbital motion. With the compensation at this “sweet spot”, the nuclear spin sees the same total magnetic field, regardless of the state of the electron, and therefore can be completely decoupled from the electronic environment [21].

In conclusion, we have shown that the vector spin-fluctuator model provides a good description for our observations of coherence properties of the optically illuminated nuclear spin qubit. Our theoretical and experimental results demonstrate a substantial suppression of nuclear spin decoherence due to the mechanism analogous to the motional averaging in NMR. Our analysis further indicated a new approach that may allow us to completely decouple the nuclear spin and the electron during optical excitation. These results are of critical importance for scalable applications of N-V-center-based quantum registers [7,8].

We thank P. Hemmer, F. Jelezko, and A. Zibrov for useful discussions and experimental help. This work was supported by NSF (CAREER and PIF programs), the ARO MURI, the Packard and Hertz Foundations.

- 
- [1] M. V. G. Dutt *et al.*, *Science* **316**, 1312 (2007).
  - [2] F. Jelezko *et al.*, *Phys. Rev. Lett.* **92**, 076401 (2004); **93**, 130501 (2004).
  - [3] D. D. Awschalom, R. J. Epstein, and R. Hanson, *Scientific American* **297**, No. 4, 84 (2007).
  - [4] L. Childress *et al.*, *Science* **314**, 281 (2006).
  - [5] T. Gaebel *et al.*, *Nature Phys.* **2**, 408 (2006).
  - [6] R. Hanson *et al.*, *Phys. Rev. Lett.* **97**, 087601 (2006).
  - [7] L. Childress *et al.*, *Phys. Rev. A* **72**, 052330 (2005); *Phys. Rev. Lett.* **96**, 070504 (2006).
  - [8] L. Jiang *et al.*, *Phys. Rev. A* **76**, 062323 (2007).
  - [9] E. Paladino *et al.*, *Phys. Rev. Lett.* **88**, 228304 (2002).
  - [10] Y. M. Galperin, B. L. Altshuler, and D. V. Shantsev, arXiv:cond-mat/031249.
  - [11] Y. M. Galperin *et al.*, *Phys. Rev. Lett.* **96**, 097009 (2006).
  - [12] J. Bergli, Y. M. Galperin, and B. L. Altshuler, *Phys. Rev. B* **74**, 024509 (2006).
  - [13] More precisely, the optical transitions involve electronic states of several electrons localized at the N-V center.
  - [14] C. P. Slichter, *Principles of Magnetic Resonance* (Springer-Verlag, Berlin, New York, 1990).
  - [15] W. Happer and A. C. Tam, *Phys. Rev. A* **16**, 1877 (1977).
  - [16] M. M. Boyd *et al.*, *Science* **314**, 1430 (2006).
  - [17] I. Reichenbach and I. H. Deutsch, *Phys. Rev. Lett.* **99**, 123001 (2007).
  - [18] P. R. Hemmer *et al.*, *Opt. Lett.* **26**, 361 (2001).
  - [19] N. B. Manson, J. P. Harrison, and M. J. Sellars, *Phys. Rev. B* **74**, 104303 (2006).
  - [20] A. Lenef and S. C. Rand, *Phys. Rev. B* **53**, 13441 (1996).
  - [21] Ionization of the N-V center caused by green light might also lead to optically induced decoherence of the nuclear spin at  $B = 0$ . Note that ionization probability should be reduced if resonant red light is used.